Monte Carlo Simulations of Pure Liquid Substituted Benzenes with OPLS Potential Functions

William L. Jorgensen,* Ellen R. Laird, Toan B. Nguyen, and Julian Tirado-Rives

Department of Chemistry, Yale University, New Haven, Connecticut 06511

Received 20 July 1992; accepted 20 August 1992

Intermolecular potential functions have been developed for use in computer simulations of substituted benzenes. Previously reported optimized potentials for liquid simulations (OPLS) for benzene and organic functional groups were merged and tested in Monte Carlo statistical mechanics simulations for the pure liquids of toluene, *m*-cresol, anisole, aniline, and benzonitrile at 25°C at 1 atm. The merged potential functions yielded acceptable thermodynamic results for the liquids except in the case of aniline, for which the error in the heat of vaporization was 12%. This was remedied by enhancing the polarity of the model to be more consistent with the observed dipole moment of aniline. Overall, the average errors in computed heats of vaporization and densities were then 2 and 1%, respectively. The structures of the liquids were characterized through energy and radial distribution functions. For *m*-cresol and aniline, the molecules participate in averages of 1.6 and 1.4 hydrogen bonds, respectively. Condensed phase effects on the torsional energies for anisole, *m*-cresol, and aniline were found to be small; *m*-cresol has a slightly enhanced tendency to be nonplanar in the liquid than in the gas phase, while anisole shows the opposite pattern.

INTRODUCTION

The importance of substituted benzenes is apparent from their common occurrence in medicinally important compounds, natural products, and receptors for organic guests.[1] In conjunction with computations of the relative binding affinities for a series of substituted benzenes with a cyclophane host,[2] we undertook the development and testing of intermolecular potential functions for substituted benzenes. Consistent with the usual procedure for generating optimized potentials for liquid simulations (OPLS) parameters,[3] emphasis was placed on reproducing experimental thermodynamic data for aqueous solutions and the pure liquids. In a previous article, relative and absolute free energies of hydration were computed via statistical perturbation theory for a series of eight mono- and disubstituted benzenes and found to be in essentially exact agreement with the available experimental data.[4] The results were in particular satisfying because the parameter assignment was simple; the Lennard–Jones parameters came directly from earlier work on benzene and the substituent groups (CH_3, OH, OCH_3, and CN) and the partial charges came from merging those for benzene, alkanes, and aliphatic alcohols, ethers, and nitriles.

The success of testing the potential functions on pure liquids is documented here. A representative for each substituent type was chosen, specifically, toluene, *m*-cresol, anisole, and benzonitrile (Scheme 1). These are all liquids at 25°C and 1 atm. *m*-Cresol was included instead of phenol because phenol's melting point is 43°C, which leads to incomplete sets of experimental thermodynamic data for the liquid at one temperature.[5] The same applies to *p*-cresol, which melts at 35°C.[5] In addition, the range of functionality from the hydration study has been expanded by the addition of aniline. The simple merger of benzene and methylamine parameters is found to be less viable in this case, so an alternative charge distribution is reported that yields improved thermodynamic results for liquid aniline. The structures of the liquids are also characterized through energy and radial distribution functions. In particular, the hydrogen bonding in liquid *m*-cresol and aniline is addressed.

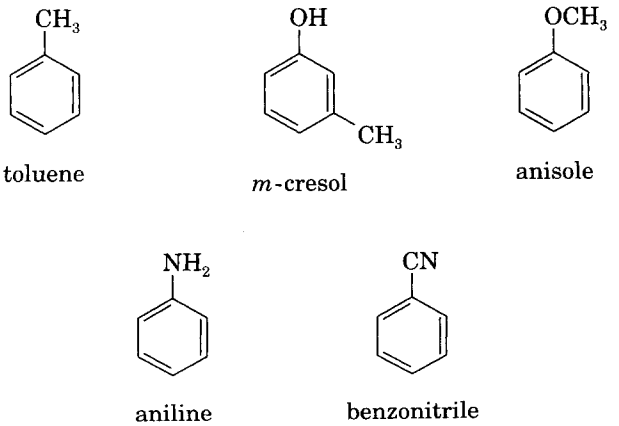

toluene — *m*-cresol — anisole

aniline — benzonitrile

*Author to whom all correspondence should be addressed.

CCC 0192-8651/93/020206-10

COMPUTATIONAL DETAILS

Molecular Structures and Potential Functions

An all-atom model is used for the substituted benzenes except methyl groups are treated as united atoms centered on the carbon. Standard geometries based upon experimental data have been adopted, as summarized in Table I.[6] It should be noted that the amino group in aniline is pyramidal; the HNH plane makes a 37.5° angle with the plane of the benzene ring in the lowest-energy rotamer that has the "lone-pair" eclipsing the π-orbitals.[7]

The potential energy between two molecules, ΔE_{ab}, consists of Coulomb and Lennard–Jones interactions between the atoms i on a and the atoms j on b, which are separated by a distince r_{ij} [eq. (1)].[3] Geometric combining rules are used for the Lennard–Jones parameters, ϵ and σ [eq. (2)]. The Lennard–Jones

$$\Delta E_{ab} = \sum_i \sum_j \{q_i q_j e^2/r_{ij} + 4\epsilon_{ij}[(\sigma_{ij}/r_{ij})^{12} - (\sigma_{ij}/r_{ij})^6]\} \quad (1)$$

$$\epsilon_{ij} = (\epsilon_i \epsilon_j)^{1/2}, \qquad \sigma_{ij} = (\sigma_i \sigma_j)^{1/2} \quad (2)$$

parameters are in general transferable to larger molecules from their components,[3] while the choice of partial charges for a new molecule is the main problem.

The OPLS parameters reported previously for benzene[8] and attached methyl, hydroxyl, methoxyl, and cyano groups have been used here (Table II).[4] There is no charge alternation in the benzene rings for the substituted systems in this simple model.[4] All unsubstituted benzene carbons and hydrogens have the same partial charges (± 0.115 e) as in benzene itself. For aniline, the same approach was tried by combining the charges for benzene and methylamine.[3b] For methylamine, the OPLS charges are 0.200, −0.900, and 0.350 e for the CH_3 group, N, and H, respectively. Combination with the benzene charges would then lead to charges for aniline of 0.085, −0.785, and 0.350 for the *ipso* carbon, N, and H, respectively. The Lennard–Jones parameters have been taken directly from benzene and methylamine. In a Monte Carlo simulation, this charge distribution yielded a density for liquid aniline within 1% of the experimental value at 25°C; however, the heat of vaporization, ΔH°_{vap}, was too low by 12%. The simple charge model is not polar enough, as reflected in its dipole moment of 1.17 D, considerably less than the experimental gas-phase value of 1.53 D.[9] Small adjustments to the charges for aniline were then made, returning the charge on N to −0.900 e and increasing the charges on the amino hydrogens to 0.400 e, which improved the heat of vaporization. The complete set of OPLS parameters used here is summarized in Table II. The partial charge distributions along with the standard geometries yield the dipole moments listed in Table III. Exact accord between the OPLS and experimental dipole moments is not sought in view of the limitations of the partial charge representation

Table I. Standard geometric parameters for substituted benzenes.

C═C	1.400
C—H	1.080
C—O	1.360
C—CN	1.451
C—CH_3	1.510
C—NH2	1.402
N—H	1.001
O—H	0.960
O—CH_3	1.430
C≡N	1.158
⟨CCC	120.0
⟨CCH	120.0
⟨CCO	120.0
⟨COH	109.0
⟨$COCH_3$	117.0
⟨CC≡N	180.0
⟨CNH	115.9
⟨HNH	113.1

Bond lengths in Å, bond angles in degrees.

Table II. OPLS parameters for substituted benzenes.

Atom	Example	q (e)	σ (Å)	ϵ (kcal/mol)
C	Benzene	−0.115	3.550	0.070
H	Benzene	0.115	2.420	0.030
CH_3	Toluene	0.115	3.800	0.170
O(H)	Phenol	−0.585	3.070	0.170
H(O)	Phenol	0.435	0.000	0.000
C(OH)	Phenol	0.150	3.550	0.070
O(R)	Anisole	−0.385	3.000	0.170
CH_3(O)	Anisole	0.250	3.800	0.170
C(OR)	Anisole	0.135	3.550	0.070
N(H_2)	Aniline	−0.900	3.250	0.170
H(N)	Aniline	0.400	0.000	0.000
C(NH_2)	Aniline	0.100	3.550	0.070
C(≡N)	Benzonitrile	0.395	3.650	0.150
N(≡C)	Benzonitrile	−0.430	3.200	0.170
C(CN)	Benzonitrile	0.035	3.550	0.070

Table III. Dipole moments for substituted benzenes.

	Dipole moment (D)	
Compound	OPLS	Experimental[a]
Toluene	0.24	0.36
Phenol	2.11	1.45
m-Cresol	2.17	
p-Cresol	2.22	1.71
Anisole	1.68	1.38
Aniline	1.35	1.53
Benzonitrile	3.23	4.18

[a]Ref. 9.

Table IV. Energetic results (kcal/mol) for liquid substituted benzenes at 25°C and 1 atm.

Liquid	$-E_i$	E_{intra} (g)	E_{intra} (l)	ΔH°_{vap} Calculated	ΔH°_{vap} Experimental[a]
Benzene	7.46 ± 0.01	0.0	0.0	8.05 ± 0.01	8.09
Toluene	8.36 ± 0.02	0.0	0.0	8.95 ± 0.02	9.08
m-Cresol	14.78 ± 0.05	0.34	0.45 ± 0.01	15.27 ± 0.05	14.75
Anisole	10.82 ± 0.02	0.36	0.29 ± 0.00	11.48 ± 0.02	11.20
Aniline	12.97 ± 0.02	0.34	0.30 ± 0.00	13.60 ± 0.02	13.34
Benzonitrile	11.96 ± 0.03	0.0	0.0	12.55 ± 0.03	12.54

E_i is the computed intermolecular potential energy for the liquid. E_{intra} is the computed torsional energy for the ideal gas (*g*) or liquid (l).
[a]Refs. 5 and 13.

and the desire to focus on reproducing fluid properties. The OPLS dipole moments for the aromatic ethers and alcohols are higher than the experimental values, similar to the situation with the aliphatic analogs,[3] while the OPLS dipole moments for the nitrogen-containing systems are lower than the experimental ones.

Monte Carlo Simulations

Monte Carlo statistical mechanics simulations were carried out for the five pure liquids in the isothermal–isobaric (NPT) ensemble at 25°C and 1 atm with Metropolis sampling. The systems consisted of 128 molecules in a cubic cell ca. 30 Å on a side with periodic boundary conditions. Each simulation began from a configuration obtained by mapping onto a configuration of an earlier simulation with structurally similar molecules, e.g., toluene from benzene[8] and *m*-cresol from toluene. An equilibration period then ensued that covered 1.0×10^6 to 4.0×10^6 configurations, during which the total energy and volume stabilized. The averaging for computed properties and distribution functions was then performed over the next 3.0×10^6 configurations.

The geometries of the molecules were not altered during the simulations except the torsional motion for the methoxy methyl group in anisole, the hydroxyl hydrogen in *m*-cresol, and the amino group in aniline was included. A twofold torsional energy term [eq. (3)] was used with V_2 values of 2.20, 3.50,

$$V(\phi) = (V_2/2)(1 - \cos 2\phi) \qquad (3)$$

and 3.54 kcal/mol for anisole, *m*-cresol, and aniline, respectively, which come from spectroscopic measurements and ab initio calculations.[10] For anisole, the dihedral angle ϕ is defined as C-C-O-C, while it is C6-C1-O-H for *m*-cresol. For aniline, a dummy atom *X* was placed in a lone-pair position on the nitrogen. The dihedral angle was then C-C-N-*X* and the phase in eq. (3) was changed by making the minus sign plus. Thus, for $\phi = 0°$ the lone-pair is in the ring plane and the energy is at the maximum, V_2, and for $\phi = 90°$ $V(\phi) = 0$.

The intermolecular interactions were spherically truncated at 13 Å based upon the distance between *ipso* (C1) carbons. A correction was made during the simulations for the Lennard–Jones interactions neglected beyond the cutoff, which lowers the total energy by 2–3% and has small effects on all other computed properties.[11] A generally accepted procedure has not emerged to correct for the Coulombic interactions beyond the cutoff. However, the lack of significant size dependence for many computed properties of liquid water may be noted.[12] New configurations were generated by randomly selecting a molecule, randomly translating it in all three Cartesian directions, rotating it randomly about a randomly chosen Cartesian axis, and performing the internal rotations for anisole, *m*-cresol, and aniline by a random amount. The translations and rotations were made within bounds of $\pm\Delta r$, $\pm\Delta\Theta$, and $\pm\Delta\phi$, which were ca. ±0.10 Å, ±10°, and ±10°, respectively. Volume changes were attempted every 1500 configurations within ranges of ±300 Å^3 by scaling the intermolecular separations. These ranges led to overall acceptance rates of about 40% for new configurations.

RESULTS AND DISCUSSION

Thermodynamics

The total energy of the liquid consists of the intermolecular potential energy, E_i, and the intramolecular torsional energy, E_{intra}. The heat of vaporization

Table V. Heat capacities (cal/mol-deg) for substituted benzenes at 25°C and 1 atm.

Liquid	$C_P^\circ(g)$[a]	$C_P^{inter}(l)$[b]	$C_P(l)$ Calculated	$C_P(l)$ Experimental[a]
Benzene	19.5	13.7	31.2 ± 1.0	32.5
Toluene	24.8	12.4	35.2 ± 1.2	37.6
m-Cresol	29.8	27.6	55.4 ± 6.3	53.8
Anisole	31.1[c]	14.5	43.6 ± 1.7	45.7
Aniline	25.9	13.3	37.2 ± 1.2	45.7
Benzonitrile	26.1	21.3	45.4 ± 3.3	45.5

[a]Ref. 5.
[b]The calculated uncertainties for C_P^{inter} are the same as for $C_P(l)$.
[c]Ref. 15.

Table VI. Molecular volumes and densities for liquid substituted benzenes at 25°C and 1 atm.

	V (Å^3)		d (g/cm^3)	
Liquid	Calculated	Experimental[a]	Calculated	Experimental[a]
Benzene	148.6 ± 0.2	148.4	0.873 ± 0.001	0.874
Toluene	175.6 ± 0.3	177.4	0.871 ± 0.001	0.862
m-Cresol	176.4 ± 0.1	174.3	1.018 ± 0.001	1.030
Anisole	181.0 ± 0.3	181.5	0.992 ± 0.002	0.989
Aniline	149.3 ± 0.2	152.0	1.036 ± 0.002	1.018
Benzonitrile	172.0 ± 0.3	171.1	0.995 ± 0.002	1.001

[a]Ref. 5.

to the ideal gas phase is then given by eq. (4). For the present cases, the heats of vaporization to the

$$\Delta H^\circ_{vap} = E_{tot}(g) - E_{tot}(1) + RT = E_{intra}(g) - E_i(1) - E_{intra}(1) + RT \quad (4)$$

ideal gas and to the real gas are the same (the enthalpy departure function, $H^\circ - H^g_{sat}$, ≈ 0) because the temperature for the simulations, 25°C, is far below the boiling points of the liquids, 100–200°C.[13] The computed and experimental results are compared in Table IV; the average error is 2% for the computed heats of vaporization. It is difficult to improve on this because the uncertainties in some of the experimental values are as much as 0.25 kcal/mol or 2%.[14] The statistical uncertainties that are shown with computed quantities are $\pm 1\sigma$ and were obtained from the fluctuations in averages over subsets 2×10^5 configurations. Results from the earlier study of liquid benzene[8] are also included in Tables IV–VI.

The distributions of total intermolecular interaction energies for molecules in the liquids are shown in Figure 1. The averages of these distributions are equal to twice the E_i values in Table IV. The molecules in the liquids experience a range of energetic environments spanning 10–25 kcal/mol. The broadest distributions are for the liquids in which hydrogen bonding is possible, *m*-cresol and aniline. The

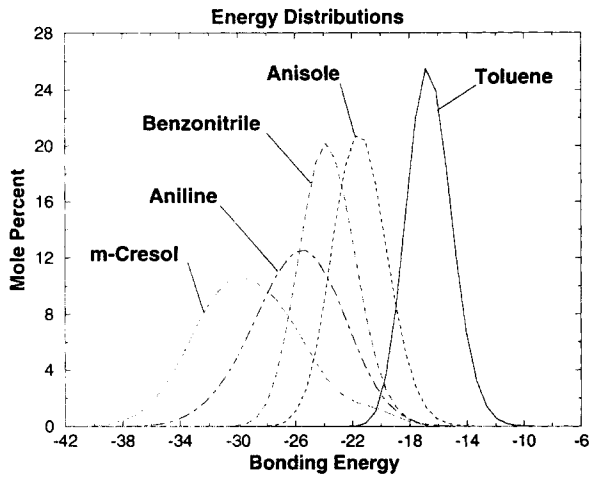

Figure 1. Computed distributions of total intermolecular interaction energies for monomers in the liquids. Units for the ordinate are mole percent per kcal/mol.

distribution for *m*-cresol is the only one distinctly bimodal. There is a small band centered at the high energy end near −22 kcal/mol. The same feature was obtained from the simulations of aliphatic alcohols,[3c] and is assigned to molecules in 0 or 1 hydrogen bond. The majority of alcohol molecules participate in two hydrogen bonds and give rise to the main band.

The energy distributions are also the primary contributors to the intermolecular component of the heat capacities according to eq. (5). The

$$C_P^{inter}(1) = [\langle (E_i + PV)^2 \rangle - \langle E_i + PV \rangle^2]/Nk_BT \quad (5)$$

contributions of the PV term to the liquid's enthalpy and of its fluctuation to the heat capacity are negligible at 1 atm. The total heat capacity of the liquid is obtained from C_P^{inter} plus the unimolecular contribution, estimated from the heat capacity of the ideal gas, $C_P^\circ(g)$, less R to remove the PV component for the ideal gas. The results are summarized in Table V. The computed heat capacities converge more slowly than the energies; however, the precision is in general reasonable from simulations of the present length.[16] The calculated results agree well with the experimental values in view of the statistical uncertainties; the average error is 6%. More precise computed values could be obtained by running simulations at different temperatures via $C_P = (\delta H/\delta T)_P$ in view of the small uncertainties in the computed energies or enthalpies. The computed intermolecular component of C_P for aniline should be larger and probably reflects particularly slow convergence in this case. The hydrogen bonding in *m*-cresol and aniline and the strong dipole–dipole interactions in benzonitrile lower the energies for these liquids, broaden their energy distributions, and increase the intermolecular components of the heat capacities.

Standard fluctuation formulas involving the volume and enthalpy were also used to compute the isothermal compressibility (k) and coefficient of thermal expansion (α).[16] These properties, in particular α, converge slowly. The computed ks in units of 10^{-6} atm^{-1} are 91 ± 6 for benzene, 77 ± 7 for toluene, 52 ± 8 for *m*-cresol, 54 ± 6 for anisole, 37 ± 4 for aniline, and 56 ± 6 for benzonitrile. Ex-

perimental data at 25°C and 1 atm appear to be available only for benzene (97.9) and toluene (92.3)[5] The computed αs in units of 10^{-5} deg^{-1} are all 50–120 with uncertainties of 10–20. This overlaps the range of experimental αs for these liquids.[5] More precise computed results could again be obtained from running simulations at different temperatures.

Another energetic issue concerns potential solvent effects on the torsional profiles for *m*-cresol, anisole, and aniline. The average torsional energies for the ideal gas phase, $E_{intra}(g)$, were obtained directly from Boltzmann distributions for the torsional potentials, eq. (3). As shown in Table IV, the torsional energies are similar in the gas and liquid phases. Nevertheless, *m*-cresol does show the greatest variation with a higher liquid-phase torsional energy. The implied greater population of out-of-plane geometries is fully consistent with the earlier investigations of *p*-cresol and phenol in water, which found that hydrogen bonding is promoted by this change.[4] Presumably, the hydroxylic hydrogen becomes less sterically hindered by the out-of-plane rotation. The computed population distributions, $S(\phi)$, for the dihedral angle in the three systems are shown in Figures 2–4. The simulations were all initiated with every dihedral angle set to zero. This bias has not fully worn off during the simulation of anisole, as evidenced by the asymmetry in the liquid $S(\phi)$ in Figure 2. For *m*-cresol, there could be an intrinsic preference in the liquid for geometries with the hydroxyl hydrogen either *syn* (ϕ = 180°) or *anti* (ϕ = 0°) to the methyl group. However, this is a remote effect, and the asymmetry in Figure 3 most likely comes from the initial bias for ϕ = 0°. In the case of aniline, there is negligible difference between the ideal gas and liquid $S(\phi)$s in Figure 4. The symmetry in the liquid-phase results was aided by the change in definition of the dihedral angle. The initial value of ϕ = 0° corresponds to the maximum for aniline and there is an equal probability of falling from there into either torsional well centered at 90 or 270°. In all cases, the interconversions between conformers could be enhanced via umbrella sampling techniques that would be essential for less symmetrical systems.[17]

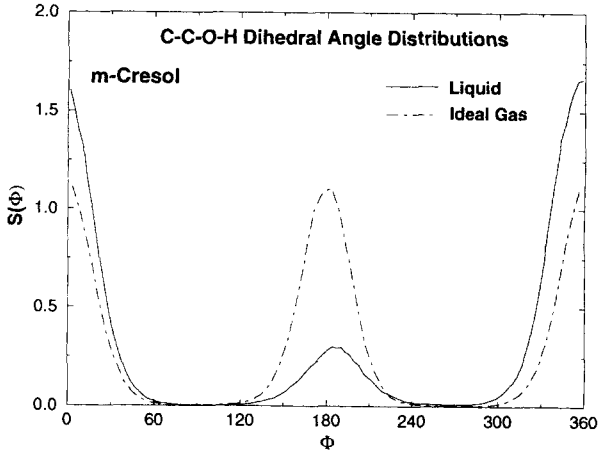

Figure 3. Computed C-C-O-H dihedral angle distributions for *m*-cresol in the ideal gas and liquid phases. ϕ = 0 and 180° correspond to the hydroxyl hydrogen being *anti* and *syn* to the methyl group.

Finally, the computed molecular volumes and, equivalently, the densities are compared with experimental data in Table V. The potential functions yield an average error of less than 1%. This supports the model, as well as the general transferability of Lennard–Jones parameters, because the densities are clearly affected by the choice of σs.

The key point from the comparisons above is that the present model for substituted benzenes, despite its simplicity, provides an accurate description of basic thermodynamic properties of the pure liquids. The excellent accord between the computed and experimental free energies of hydration is also notable.[4]

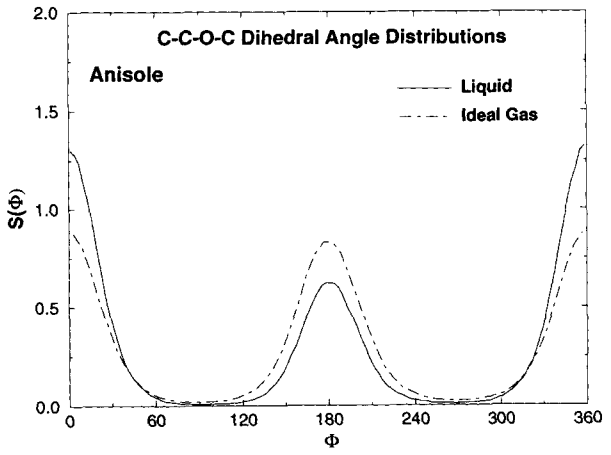

Figure 2. Computed C-C-O-C dihedral angle distributions for anisole in the ideal gas and liquid phases. Units for the ordinate are mole percent per degree.

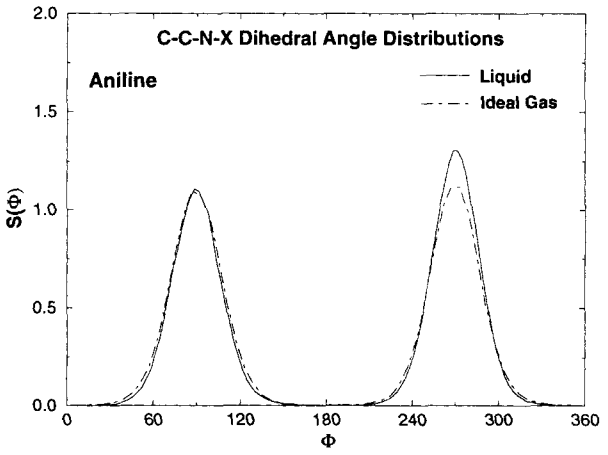

Figure 4. Computed C-C-N-*X* dihedral angle distributions for aniline in the ideal gas and liquid phases. *X* is on the bisector of the HNH angle.

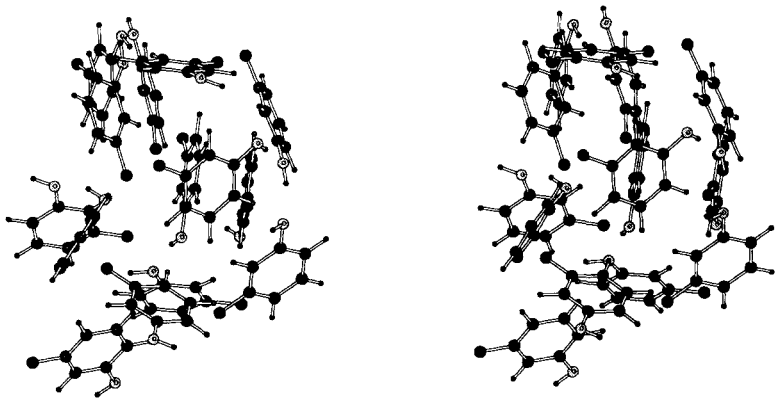

Figure 5. Stereoplot of a molecule near the center of the simulation cell and its nearest neighbors in liquid *m*-cresol.

Radial Distribution Functions, Liquid Structure, and Hydrogen Bonding

The structures of the liquids can be visualized by displaying configurations from the simulations. In liquid and solid benzene, simulations and experiments find 12 nearest neighbors for each molecule with edge-to-face and offset-stacked arrangements predominating.[8] This remains the basic theme for the liquid substituted benzenes with 12–13 nearest neighbors in each case. The stereoplots in Figure 5 for *m*-cresol and Figure 6 for aniline are illustrative. For clarity, only one molecule near the center of the periodic box is shown with its nearest neighbors that have at least one interatomic contact of 5 Å or less. The packing of the benzene rings is still a dominant issue; however, for the polar substituted systems attractive interactions between the substituents are also well accommodated. This is further addressed below through radial distribution functions (rdfs) and energy pair distributions. The rdf $g_{xy}(r)$ gives the probability of occurrence of an atom of type y at a distance r from an atom of type x, normalized for the bulk density of the liquid. Peaks in rdfs are associated with solvation shells or specific neighbors and can be integrated to yield coordination numbers. The focus here is on the rdfs involving the atoms of the substituents. The energy pair distributions show the spectrum of individual molecule–molecule interactions in the liquids and can give insights on strong interactions such as hydrogen bonding.

For toluene, the CH_3—CH_3, C1—CH_3, and C1—C1 rdfs are shown in Figure 7, while the CH_3—CH_3, O—CH_3, and O—O rdfs for anisole are in Figure 8 and the N—N, C(N)—N, and C(N)—C(N) rdfs for benzonitrile are in Figure 9. Most of these rdfs show broad first peaks ranging from the shortest contacts near 3 Å to the minima near 6–7 Å. In every case, the integrals of these rdfs to 6 Å and 7 Å are 4–5 and 7–8, which reflect fundamental packing requirements. Some enhanced order for the more polar systems is apparent relative to toluene. For example, in liquid anisole (Fig. 8) electrostatic effects account for moving the first peak of the O—O rdf to 5 Å, while the O—CH_3 rdf shows significantly greater population in the 3- to 4-Å area. The double peak from 3–6 Å in the O—CH_3 rdf is characteristic of liquid ethers; the oxygen is particularly close, 3–4 Å, to one α-carbon and the other α-carbon contributes to the second peak near 5 Å.[18] For anisole, the first peak in the O—CH_3 rdf integrates to 0.8 out to 4 Å,

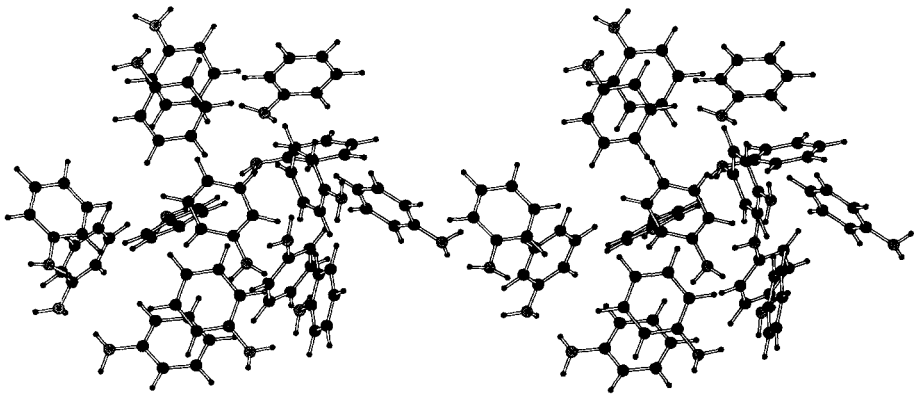

Figure 6. Stereoplot of a molecule near the center of the simulation cell and its nearest neighbors for liquid aniline.

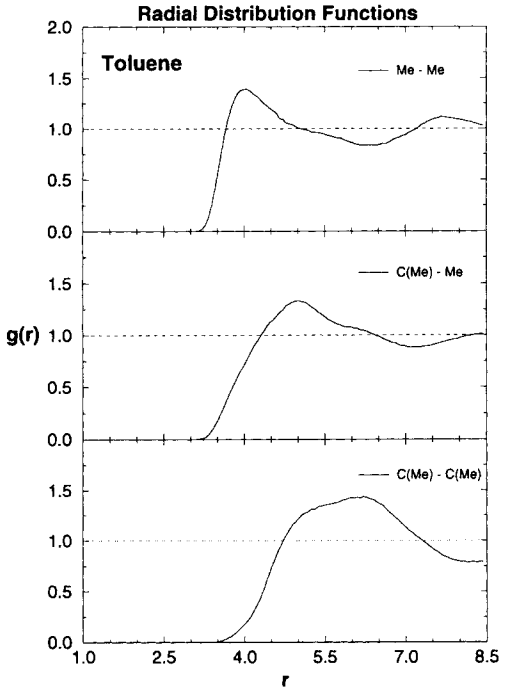

Figure 7. Computed Me—Me C(Me)—Me, and C(Me)—C(Me) radial distribution functions for liquid toluene. Me refers to the carbon of the methyl group and C(Me) is the attached carbon atom.

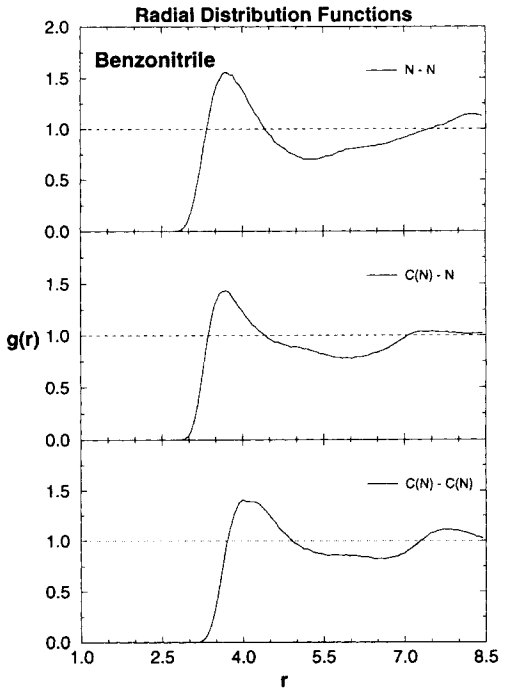

Figure 9. Computed N—N, C(N)—N, and C(N)—C(N) radial distribution functions for liquid benzonitrile. C(N) is the carbon in the cyano group.

so there are 1.6 of these short contacts for each molecule in the liquid. Further, in the case of benzonitrile the rdfs in Figure 9 are reminiscent of the analogous rdfs for liquid acetonitrile.[19] In that study, the influence of the electrostatic interactions on the rdfs was shown to be dramatic by running a simulation at the same density with all partial charges set to zero.[19]

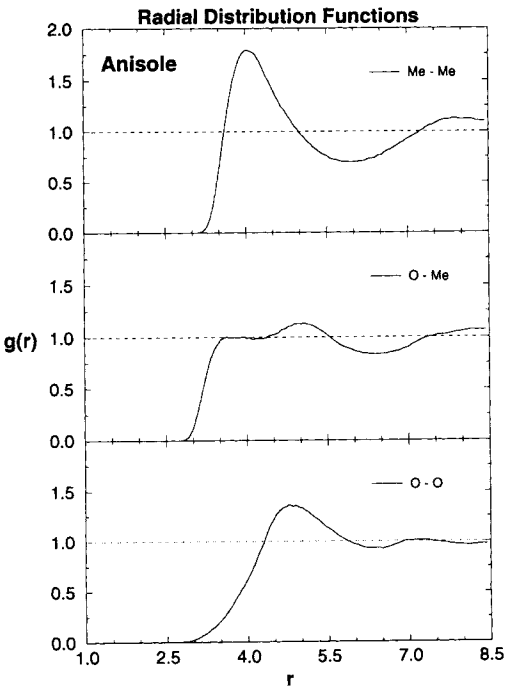

Figure 8. Computed Me—Me, O—Me, and O—O radial distribution functions for liquid anisole.

Nevertheless, the intermolecular ordering of the substituent groups in the dipolar aprotic liquids is modest compared to liquid *m*-cresol and aniline, for which the hydrogen bonding is strikingly apparent in Figures 10–13. The sharp first peak in the O—O rdf for *m*-cresol integrates to 1.6 out to 3.5 Å (Fig. 10). This estimate of the number of hydrogen bonds per molecule is confirmed by the sharp first peak in the O—H rdf that has an integral of 0.8 out to 2.5 Å. Thus, an oxygen has an average of 0.8 hydrogen-bonded hydrogen, and the hydroxyl hydrogen on the oxygen averages 0.8 hydrogen-bonded oxygen neighbor to total 1.6 hydrogen bonds per molecule. The integral of the first peak in the C1—O rdf in Figure 11 is 1.8 to the minimum at 4.2 Å; however, the best estimate of the number of hydrogen bonds comes from the O—H rdf, which does not integrate to 0.9 until 3.0 Å. The two peaks in the C1—H rdf (Fig. 11) are also typical of alcohols;[3c] the first peak integrates to 0.9 at 3.4 Å and contains the hydrogen from a hydrogen bond-donating neighbor, while the second peak is for the hydrogen on a hydrogen bond-accepting neighbor as is the second peak in the O—H rdf. The number of hydrogen bonds is lower than the 1.8–1.9 that has been obtained in simulations of liquid aliphatic alcohols including isopropanol and 2-methyl-2-propanol.[3c] Thus, it is apparently more difficult to accommodate simultaneously the hydrogen bonding and packing of phenyl rings than *t*-butyl groups.

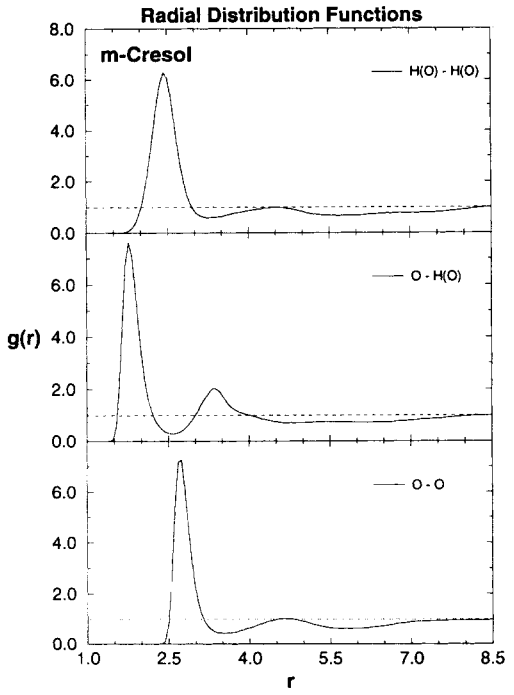

Figure 10. Computed H(O)—H(O), O—H(O), and O—O radial distribution functions for liquid *m*-cresol. H(O) is the hydroxyl hydrogen.

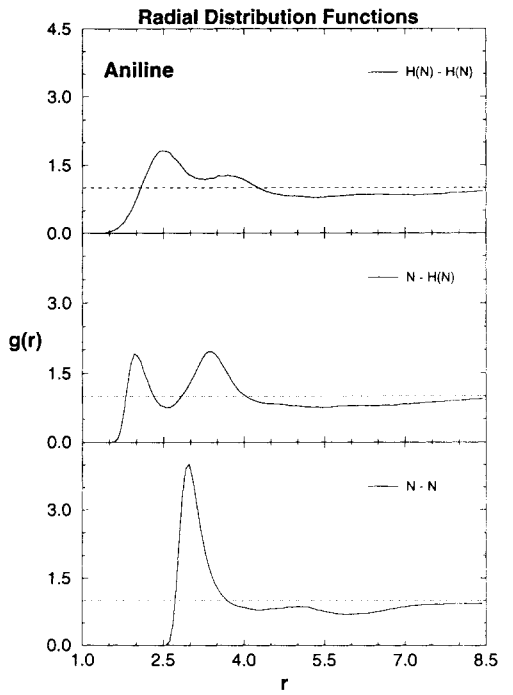

Figure 12. Computed H(N)—H(N), N—H(N), and N—N radial distribution functions for liquid aniline. H(N) is an amine hydrogen.

The hydrogen bonding is also obvious in the rdfs for aniline (Figs. 12 and 13), although not as striking as for *m*-cresol based upon the peak heights. The first peak in the N—N rdf in Figure 12 has its maximum at 3.0 Å and integrates to 1.65 at 3.5 Å. The number of hydrogen bonds is better defined by the well-resolved first peak in the N—H rdf; integration to the minimum at 2.55 Å yields 0.7 hydrogen-bonded hydrogen for each nitrogen and 1.4 hydrogen bonds per molecule overall. The second peak in the N—H

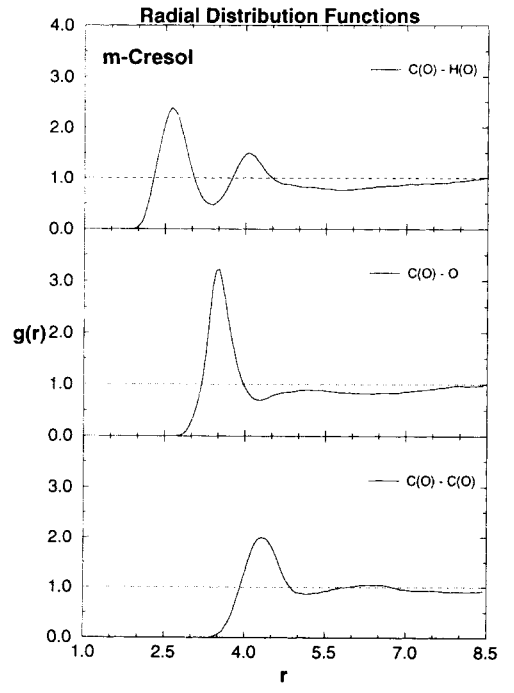

Figure 11. Computed C(O)—H(O), C(O)—O, and C(O)—C(O) radial distribution functions for liquid *m*-cresol. C(O) is the carbon bonded to oxygen.

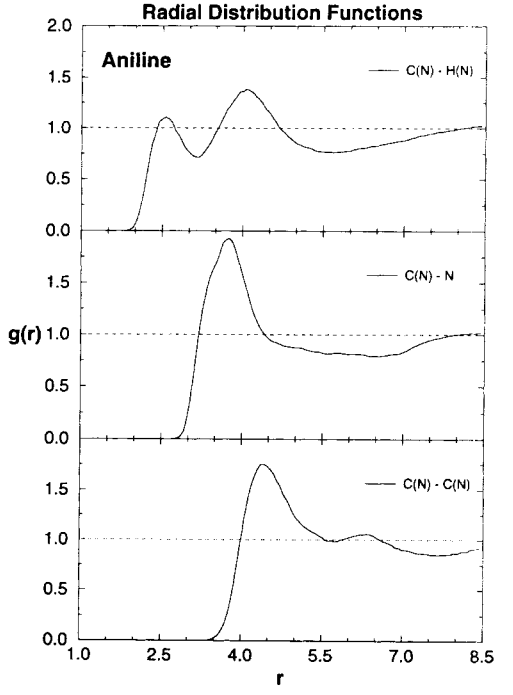

Figure 13. Computed C(N)—H(N), C(N)—N, and C(N)—C(N) radial distribution functions for liquid aniline. C(N) is the carbon bonded to nitrogen.

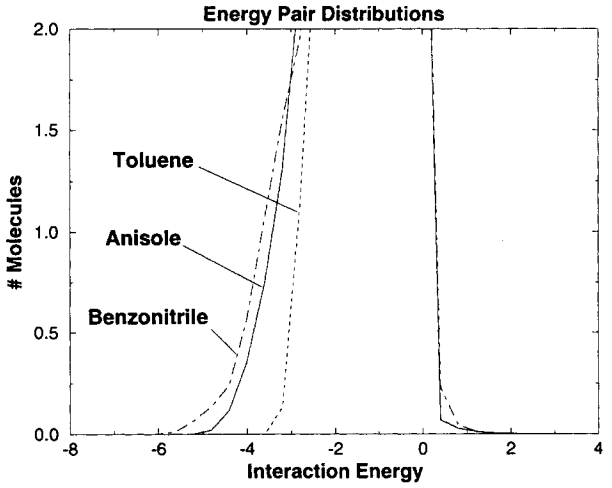

Figure 14. Computed distributions of individual intermolecular interaction energies in liquid toluene, anisole, and benzonitrile. Units for the ordinate are number of molecules per kcal/mol.

rdf, which extends to about 4 Å, includes the two hydrogens from a hydrogen bond-accepting neighbor and the non-hydrogen-bonded hydrogen from hydrogen bond-donating neighbors. The two peaks in the C1—H rdf in Figure 13 can be assigned the same way; the first peak out to 3 Å contains the donating hydrogens and integrates to 0.85.

The difference between the hydrogen-bonded liquids and the others is also apparent in the energy pair distributions in Figures 14 and 15. For *m*-cresol and aniline, the hydrogen-bonded neighbors stand out in the low-energy bands from −8 to −4 kcal/mol (Fig. 15). Quite consistent with the information from the rdfs, these bands integrate to 1.7 hydrogen bonds for *m*-cresol and 1.1 for aniline, in which case the integration limit is less clear. Extending the integration to −3.6 kcal/mol yields 1.6 interactions for aniline and 1.9 for *m*-cresol. Toluene and anisole

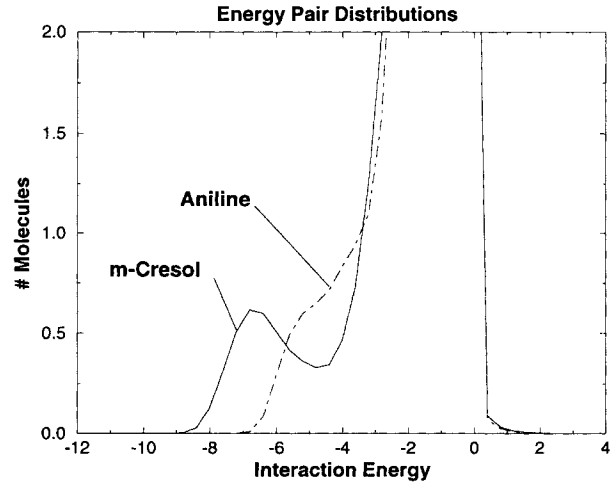

Figure 15. Computed distributions of individual intermolecular interaction energies in liquid *m*-cresol and aniline.

have no intermolecular interactions more attractive than −3.5 and −5.0 kcal/mol, respectively. The range extends to 5.8 kcal/mol for the more dipolar benzonitrile; however, the most attractive interactions for these three liquids just merge into the bulk spike centered at 0 kcal/mol in Figure 14. Thus, the range of individual interactions is greater for the hydrogen-bonded liquids and extends to lower energies, which leads to lower intermolecular energies and higher intermolecular heat capacities.

The hydrogen bonding in liquid *m*-cresol and aniline is also illustrated in the stereoplots in Figures 5 and 6. In these and other plots of configurations, molecules in no hydrogen bonds are rare. Multimers, sometimes cyclic, are evident with the common occurrence of trimers and tetramers, although a quantitative analysis of their frequency has not been performed.

CONCLUSION

Intermolecular potential functions for substituted benzenes have been developed and shown to exhibit good success in reproducing experimental densities and heats of vaporization of pure liquids. The prior results for free energies of hydration[4] further support the quality of the model. The transferability of Lennard–Jones parameters from aliphatic to aromatic systems is not problematic and the use of merged charges is often viable. However, the results for aniline demonstrate the need to perform supporting fluid-phase calculations to guarantee the appropriateness of the partial charges for a new system. The Monte Carlo simulations also helped characterize the structures of the liquid substituted benzenes including the differences between dipolar aprotic and hydrogen-bonded liquids.

Gratitude is expressed to the National Science Foundation and the National Institutes of Health for support of this research.

References

1. F. Diederich, *Cyclophanes, Monographs in Supramolecular Chemistry*, Vol. 2, J.F. Stoddart, Ed., Royal Society of Chemistry, Cambridge, UK, 1991; R.S. Silverman, *The Organic Chemistry of Drug Design and Drug Action*, Academic Press, New York, 1992.
2. W.L. Jorgensen, T.B. Nguyen, E.M. Sanford, I. Chao, K.N. Houk, and F. Diederich, *J. Am. Chem. Soc.*, **114,** 4003 (1992).
3. (a) W.L. Jorgensen and J. Tirado-Rives, *J. Am. Chem. Soc.*, **110,** 1657 (1988); (b) W.L. Jorgensen, J.M. Briggs, and L. Contreras, *J. Phys. Chem.*, **94,** 1683 (1990); (c) W.L. Jorgensen, *J. Phys. Chem.*, **90,** 1276 (1986).
4. W.L. Jorgensen and T.B. Nguyen, *J. Comp. Chem.*, **14,** 195 (1993).
5. J.A. Riddick, W.B. Bunger, and T.K. Sakano, *Organic Solvents*, 4th Ed., Wiley-Interscience, New York, 1986;

J.D. Cox and G. Pilcher, *Thermochemistry of Organic and Organometallic Compounds*, Academic Press, New York, 1970.
6. M.D. Harmony, V.W. Laurie, R.L. Kuczkowski, R.H. Schwendeman, D.A. Ramsay, F.J. Lovas, W.J. Lafferty, and A.G. Maki, *J. Phys. Chem. Ref. Data*, **8,** 619 (1979); G.M. Anderson, P.A. Kollman, L.N. Domelsmith, and K.N. Houk, *J. Am. Chem. Soc.*, **101,** 2344 (1979).
7. D.G. Lister, J.K. Tyler, J.H. Hog, and N.W. Larsen, *J. Mol. Struct.*, **23,** 253 (1974); D.A. Smith, C.W. Ulmer II, and M.J. Gilbert, *J. Comp. Chem.*, **13,** 640 (1992).
8. W.L. Jorgensen and D.L. Severance, *J. Am. Chem. Soc.*, **112,** 4768 (1990).
9. R.D. Nelson, D.R. Lide, and A.A. Maryott, *Natl. Std. Ref. Data Serv., Natl. Bur. Std. US*, **10,** 1 (1967).
10. J.C. Evans, *Spec. Acta*, **16,** 428 (1960); L. Radom, W.J. Hehre, J.A. Pople, G.L. Carlson, and W.G. Fateley, *J. Chem. Soc. Chem. Commun.*, 308 (1972); D.C. Spellmeyer, P.D.J. Grootenhuis, M.D. Miller, L.F. Kuyper, and P.A. Kollman, *J. Phys. Chem.*, **94,** 4483 (1990).
11. W.L. Jorgensen, J.D. Madura, and C.J. Swenson, *J. Am. Chem. Soc.*, **106,** 6638 (1984).
12. W.L. Jorgensen and J.D. Madura, *Mol. Phys.*, **56,** 1381 (1985).
13. V. Majer and V. Svoboda, *Enthalpies of Vaporization of Organic Compounds, IUPAC Chemical Data Series No. 32*, Blackwell Scientific Publications, Oxford, UK, 1985, p. 59.
14. R.J.L. Andon, D.P. Biddiscombe, J.D. Cox, R. Handley, D. Harrop, E.F.G. Herrington, and J.F. Martin, *J. Chem. Soc.*, 5246 (1960).
15. J.L. Hales, E.B. Lees, and D.J. Ruxton, *Trans. Faraday Soc.*, **63,** 1876 (1967).
16. W.L. Jorgensen, *Chem. Phys. Lett.*, **92,** 405 (1982).
17. W.L. Jorgensen, *J. Phys. Chem.*, **87,** 5304 (1983).
18. J.M. Briggs, T. Matsui, and W.L. Jorgensen, *J. Comp. Chem.*, **11,** 958 (1990).
19. W.L. Jorgensen and J.M. Briggs, *Mol. Phys.*, **63,** 547 (1988).